IEEE Access
Multidisciplinary | Rapid Review | Open Access Journal

Received March 30, 2019, accepted April 23, 2019, date of publication May 7, 2019, date of current version May 21, 2019.

Digital Object Identifier 10.1109/ACCESS.2019.2915189

Grid-Free DOD and DOA Estimation for MIMO Radar via Duality-Based 2D Atomic Norm Minimization

WEN-GEN TANG, (Student Member, IEEE), HONG JIANG, (Member, IEEE), AND SHUAI-XUAN PANG

College of Communication Engineering, Jilin University, Changchun 130012, China

Corresponding author: Hong Jiang (jiangh@jlu.edu.cn)

This work was supported in part by the National Natural Science Foundation of China under Grant 61371158 and Grant 61771217, and in part by the Jilin Provincial Natural Science Foundation of China under Grant 20180101329JC.

ABSTRACT Atomic norm minimization (ANM) has recently become a powerful tool for gridless compressed sensing (CS). In this paper, the issue of joint estimation of direction-of-departure (DOD) and direction-of-arrival (DOA) for bistatic multiple-input-multiple-output (MIMO) radar is investigated via two dimensional (2D) ANM. However, a major problem of the primal 2D-ANM is that the direct conversion of 2D-ANM into its semi-definite programming (SDP) problem is not strictly established theoretically and is just an approximation, which results in a decline in estimation performance. Besides, the primal 2D-ANM is limited to a single measurement vector (SMV) model. We propose a duality-based 2D-ANM algorithm for grid-free DOD and DOA estimation in MIMO radar, in which the 2D-ANM problem is effectively solved over its optimal variables in the dual-domain with SDP. Thus it retains the benefits of 2D-ANM and holds in theory. Also, it is applicable for SMV as well as multiple measurement vectors (MMV) models and appropriate for non-uniform linear arrays. The simulation results show that the proposed algorithm avoids the grid mismatch effect in DOD and DOA estimation in contrast to the conventional CS methods, and is robust to target correlation and the single-snapshot environment in comparison with the traditional subspace methods.

INDEX TERMS Bistatic MIMO radar, DOD and DOA estimation, gridless compressed sensing, two-dimensional atomic norm minimization (2D-ANM), duality.

I. INTRODUCTION

Multiple-input multiple-output (MIMO) radar systems has potential advantages over conventional phased-array radars by transmitting multiple linearly independent waveforms and receiving signals by multiple antennas [1], which has greatly enhanced the direction-finding ability and target localization accuracy [2]–[4]. Bistatic MIMO radar with respectively closely spaced transmitters and receivers, can achieve coherent processing gain and high-resolution spatial spectral estimates [5]. Specifically, joint direction-of-departure (DOD) and direction-of-arrival (DOA) estimation in bistatic MIMO radar has become a key issue in radar signal processing and attracted lots of attention. So far, various approaches have been put forward in the field. In [6], a two dimensional (2D) Capon method has been proposed to obtain the DOD and DOA estimation. In [7], a 2D multiple signal classification (2D-MUSIC) algorithm and its reduced-dimension version have been deduced for DOD and DOA estimation. In [8], [9], the 2D estimating signal parameter via rotational invariance techniques (2D-ESPRIT) has been introduced to estimate DOD and DOA of targets. In [10], a 2D expectation-maximization (2D-EM) maximum likelihood (ML) algorithm has been used for direction finding in bistatic MIMO radar. Besides, several search-free 2D angle estimation methods have been developed [11]–[13]. Despite the fact that these methods have improved the performance of DOD and DOA estimation in bistatic MIMO radar, they depend on sample covariance matrices of the observed data. When the snapshots are not sufficient relative to the number of antennas, their estimation accuracy will degrade since the sample covariance matrices are no longer the ML estimator of their statistical

The associate editor coordinating the review of this manuscript and approving it for publication was Chenhao Qi.

covariance matrices. In addition, the subspace-based methods cannot work with a single snapshot, and fail to be applied to estimate the angles of coherent targets.

Recently, compressed sensing (CS) theory [14], [15] has drawn tremendous attention in many applications. According to the idea of CS, a spare signal can be recovered from much fewer samples than required by Nyquist sampling theory. The application of CS to MIMO radar has been explored in [16]–[19], mainly due to the fact that natural targets admit a sparse or an approximate sparse representation in a certain spatial domain. In [20], the conventional least absolute shrinkage and selection operator (LASSO) method [21] has been extended to tackle joint sparse recovery for 2D parameters of MIMO radar. However, such sparse signal recovery-based algorithms require to discretize the range of interest into a grid of spatial angles, and assume that the true angles of target should fall on the predefined grid. In some practical situations in bistatic MIMO radar, no matter how fine the grid is, the true DOD and DOA may not necessarily lie on the exact grid. The off-grid target would cause a grid-mismatch effect [22], which not only violates the sparsity conditions but also deteriorates the estimation performance.

To overcome the grid-mismatch effect, some approaches have been put forward recently. One is off-grid CS [23]–[25] methods, in which the range of angle is first discretized into a grid, then the first-order Taylor expression is used to gradually approaching the true angle of off-the-grid target. Currently, these methods are only available for one dimensional (1D) estimation. The other is grid-free CS technologies based on atomic norm minimization (ANM) [26]. ANM methods can recover the sparse signal in continuous domain without grid discretization, and has become a powerful tool for gridless CS. In [27], 1D-ANM has been applied to line spectral estimation with a single measurement vector (SMV). In [28], 1D-ANM has been used in gridless DOA estimation with gain/phase uncertainties. In [29], the line spectrum is estimated via 1D-ANM from complete and incomplete data. In [30], the 1D-ANM with multiple measurement vectors (MMV) has been explored. In [31], 2D grid-free compressive beamforming has been investigated, and a 2D-ANM method has been proposed to estimate the elevation and azimuth of the acoustic sources. However, the direct conversion of the primal 2D-ANM into its semi-definite programming (SDP) problem is not strictly established theoretically and is just an approximation [31]. Besides, the primal 2D-ANM is limited to a SMV model. These approximation and limitations will result in a decline in estimation performance.

To solve the above problem, we propose a novel duality-based 2D-ANM algorithm (we name it 2D-ANM-duality) in this paper, and apply it to the issue of grid-free DOD and DOA estimation in bistatic MIMO radar. In the proposed algorithm, we convert the primal 2D-ANM into its 2D dual problem. Thus, the problem can be effectively solved over its optimal variables in the dual domain with SDP. We derive the expression of 2D Language dual function, give its optimal solution, and construct a 2D spatial spectral function based on optimal dual variables. The proposed algorithm can retain the benefits of 2D-ANM and holds theoretically. In addition, it is applicable for SMV as well as MMV models, and appropriate for non-uniform linear array (non-ULA) case. In contrast to the conventional CS methods such as 2D-LASSO, the proposed algorithm can avoid the grid mismatch effect in DOD and DOA estimation. Also, compared with the traditional subspace methods such as 2D-MUSIC or 2D-ESPRIT, it is robust to target correlation and single-snapshot environment.

The remaining of this paper is organized as follows. In section II, the signal model for DOD and DOA estimation in bistatic MIMO radar is illustrated. In section III, the 2D ANM problem is formulated. In section IV, the primal 2D-ANM method for DOD and DOA estimation is introduced. In section V, the 2D-ANM-duality algorithm for DOD and DOA estimation is proposed. In section VI, the proposed algorithm in non-ULAs and the computational complexity are discussed. Section VII presents the numerical simulations, and Section VIII draws the conclusion of this paper.

Notations: Vectors and matrices are denoted by lowercase boldface and uppercase boldface, respectively. $\mathbf{I}_N$ denotes the $N \times N$ identity matrix. $(\cdot)^*$, $(\cdot)^T$ and $(\cdot)^H$ represent the conjugate, transpose and conjugate transpose of matrix respectively. $\otimes$ denotes the Kronecker product. $\oplus$ is the Khatri-Rao product. The notation $tr(\cdot)$ denotes the trace of a matrix. $diag(\mathbf{x})$ is a diagonal matrix with vector $\mathbf{x}$ being its diagonal and $diag(\mathbf{A}, n)$ returns a column vector of the elements on the n-th diagonal of A. $vec(\cdot)$ means the vectorization operator. $Ivec(\cdot)_{N\times M}$ means rearranging the data into an $N \times M$ matrix. $\|\cdot\|_2$ represents the ℓ_2 norm. $\|\cdot\|_\infty$ represents the infinity norm. $sum(\cdot)$ returns the sum of the elements. $inf(\cdot)$ denotes the infimum.

II. SIGNAL MODEL

In this section, we consider a bistatic MIMO radar system with the following parameters:

- P narrow-band point targets illuminated from the far field.
- M transmitting and N receiving antennas consisting of uniform linear arrays (ULA).
- M orthogonal transmitting pulse waveforms, each consisting of K codes for each pulse.
- Swerling II case in which radar cross section (RCS) is varying independently from pulse to pulse and the coherent processing interval (CPI) consists of L pulses.

The bistatic MIMO radar configuration is shown in Fig.1. d_t and d_r denote the elementary spacings of the transmitting and receiving antennas of ULA, respectively, $d_t \leq \lambda/2$ and $d_r \leq \lambda/2$, where λ is the wavelength of the transmitting waveforms. φ_i and θ_i for $i = 1, 2, \ldots, P$ denote the DOD and DOA of the i-th target, respectively.

During the l-th pulse, $l = 1, 2, \ldots, L$, the return signals at receiving array can be written as an $N \times K$ matrix

$$\mathbf{Y}_l = \mathbf{A}(\theta)diag(\mathbf{s}_l)\mathbf{B}(\varphi)^T\mathbf{W} + \mathbf{N}_l \tag{1}$$

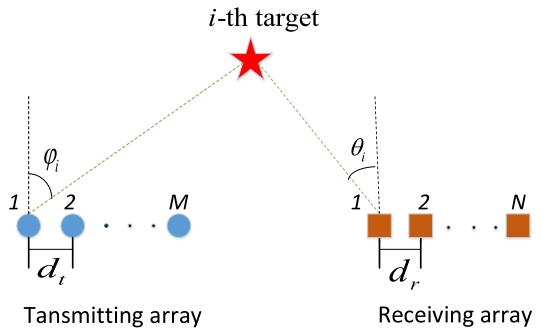

FIGURE 1. Bistatic MIMO radar configuration.

where $\mathbf{A}(\theta) = [\mathbf{a}(\theta_1), \mathbf{a}(\theta_2), \ldots, \mathbf{a}(\theta_P)] \in \mathbb{C}^{N\times P}$ and $\mathbf{B}(\varphi) = [\mathbf{b}(\varphi_1), \mathbf{b}(\varphi_2), \ldots, \mathbf{b}(\varphi_P)] \in \mathbb{C}^{M\times P}$ denote the receiving and transmitting steering matrices, respectively, where $\mathbf{a}(\theta_i) = [1, e^{-j\frac{2\pi d_r \sin(\theta_i)}{\lambda}}, \cdots, e^{-j(N-1)\frac{2\pi d_r \sin(\theta_i)}{\lambda}}]^T$ and $\mathbf{b}(\varphi_i) = [1, e^{-j\frac{2\pi d_t \sin(\varphi_i)}{\lambda}}, \cdots, e^{-j(M-1)\frac{2\pi d_t \sin(\varphi_i)}{\lambda}}]^T$. $\mathbf{s}_l = [s_{l1}, s_{l2}, \ldots, s_{lP}]^T \in \mathbb{C}^{P\times 1}$ denotes the target signal vector during the l-th pulse, where s_{li} is the complex amplitudes having time-varying characteristics during different pulses, and is proportional to the RCS of the i-th target. $\mathbf{W} = [\mathbf{w}_1, \mathbf{w}_2, \ldots, \mathbf{w}_M]^T \in \mathbb{C}^{M\times K}$ denotes the transmitting baseband coded waveform matrix, $\mathbf{w}_m \in \mathbb{C}^{K\times 1}$ belongs to the m-th transmitting antenna. The M orthogonal transmitting waveforms satisfy $\mathbf{W}\mathbf{W}^H = \mathbf{I}_M$. Finally, $\mathbf{N}_l \in \mathbb{C}^{N\times K}$ denotes the noise matrix during the l-th pulse, which is temporally and spatially white Gaussian and uncorrelated with the targets.

Applying $\mathbf{W}^H$ as the matched filter matrix, we can obtain

$$\hat{\mathbf{Y}}_l = \mathbf{Y}_l\mathbf{W}^H = \mathbf{A}(\theta)diag(\mathbf{s}_l)\mathbf{B}(\varphi)^T + \mathbf{N}_l\mathbf{W}^H \tag{2}$$

where $\hat{\mathbf{Y}}_l \in \mathbb{C}^{N\times M}$. By vectorizing the matrix $\hat{\mathbf{Y}}_l$, we can obtain the observed vector as

$$\mathbf{x}_l = vec(\hat{\mathbf{Y}}_l) = (\mathbf{B}(\varphi) \oplus \mathbf{A}(\theta))\,\mathbf{s}_l + \mathbf{n}_l \tag{3}$$

where $\mathbf{x}_l \in \mathbb{C}^{MN\times 1}$, $\mathbf{B}(\varphi) \oplus \mathbf{A}(\theta) = [\mathbf{b}(\varphi_1) \otimes \mathbf{a}(\theta_1), \mathbf{b}(\varphi_2) \otimes \mathbf{a}(\theta_2), \ldots, \mathbf{b}(\varphi_P) \otimes \mathbf{a}(\theta_P)]$, and $\mathbf{n}_l = vec(\mathbf{N}_l\mathbf{W}^H)$.

After collecting the data of L pulses, we can represent the observed signal model as

$$\mathbf{X} = (\mathbf{B}(\varphi) \oplus \mathbf{A}(\theta))\,\mathbf{S} + \mathbf{N} \tag{4}$$

where $\mathbf{X} = [\mathbf{x}_1, \mathbf{x}_2, \ldots, \mathbf{x}_L]$, $\mathbf{S} = [\mathbf{s}_1, \mathbf{s}_2, \ldots, \mathbf{s}_L]$ and $\mathbf{N} = [\mathbf{n}_1, \mathbf{n}_2, \ldots, \mathbf{n}_L]$.

III. 2D ATOMIC NORM MINIMIZATION PROBLEM

Motivated by the concept of atomic norm [32], we define the 2D atomic set of DOD and DOA as

$$\mathcal{A} \triangleq \{\mathbf{b}(\varphi) \otimes \mathbf{a}(\theta) : \varphi \in [-\pi/2, \pi/2), \theta \in [-\pi/2, \pi/2)\} \tag{5}$$

Then the 2D atomic l_0 norm of the observed vector $\mathbf{x}_l$ in (3) can be denoted as

$$\|\mathbf{x}_l\|_{\mathcal{A},0} \triangleq inf\{k : \mathbf{x}_l = \sum_{i=1}^{k} h_{li}\mathbf{b}(\varphi_i) \otimes \mathbf{a}(\theta_i), \mathbf{b}(\varphi_i) \otimes \mathbf{a}(\theta_i) \in \mathcal{A}\} \tag{6}$$

Since the solution of l_0 norm is a NP-hard problem and computationally intractable, we exploit its convex relaxation, and express the 2D atomic norm of $\mathbf{x}_l$ as

$$\|\mathbf{x}_l\|_{\mathcal{A}} \triangleq inf\{\sum_i |h_{li}| : \mathbf{x}_l = \sum_i h_{li}\mathbf{b}(\varphi_i) \otimes \mathbf{a}(\theta_i), \mathbf{b}(\varphi_i) \otimes \mathbf{a}(\theta_i) \in \mathcal{A}\} \tag{7}$$

Thus, the grid-free DOD and DOA estimation becomes a 2D atomic norm minimization problem. Its objective function is to minimize $\|\mathbf{x}_l\|_{\mathcal{A}}$, i.e.,

$$\begin{aligned} &\min_{\mathbf{h}_l, \mathbf{n}_l} \|\mathbf{x}_l\|_{\mathcal{A}} \\ &s.t.\ \mathbf{x}_l = \mathbf{U}\mathbf{h}_l + \mathbf{n}_l \\ &\quad \|\mathbf{n}_l\|_2 \le \epsilon \end{aligned} \tag{8}$$

where $\mathbf{U}_i \in \mathcal{A}$ $(i = 1, 2, \cdots)$ denotes the i-th column of $\mathbf{U}$, and $\mathbf{h}_l$ can be regarded as a sparse vector which satisfies the requirement for an accurate recovery with CS methods. ϵ denotes the noise bound.

IV. PRIMAL 2D-ANM FOR DOD AND DOA ESTIMATION

In this section, we consider applying the primal 2D-ANM method [31] to DOA and DOD estimation. This method is limited to SMV model, so the number of snapshots (pulses) is $L = 1$ for the observed matrix $\mathbf{X}$ in (4).

According to [31], (8) can be approximately casted to a semi-definite programming (SDP) problem to obtain a noise-free observation $\hat{\mathbf{X}}$, i.e.,

$$\begin{aligned} &\min_{\mathbf{u}, \hat{\mathbf{X}}, \lambda} \frac{1}{2MN} Tr(T(\mathbf{u})) + \frac{1}{2}\lambda \\ &s.t. \begin{bmatrix} T(\mathbf{u}) & \hat{\mathbf{X}} \\ \hat{\mathbf{X}}^H & \lambda \end{bmatrix} \ge 0, \quad \|\hat{\mathbf{X}} - \mathbf{X}\|_2 \le \epsilon \end{aligned} \tag{9}$$

where $\mathbf{u} = [u_{0,0}, u_{0,1}, \ldots, u_{0,N-1}, u_{1,-(N-1)}, u_{1,-(N-2)}, \ldots, u_{1,(N-1)}, u_{M-1,-(N-1)}, u_{M-1,-(N-2)}, \ldots, u_{M-1,(N-1)}] \in \mathbb{C}^{N_u}$, where $N_u = (M-1)(2N-1) + N$, $T(\mathbf{u})$ maps $\mathbf{u}$ into a Hermitian, twofold block Toeplitz matrix

$$T(\mathbf{u}) = \begin{bmatrix} \mathbf{T}_0 & \mathbf{T}_1 & \cdots & \mathbf{T}_{M-1} \\ \mathbf{T}_1^H & \mathbf{T}_0 & \cdots & \mathbf{T}_{M-2} \\ \vdots & \vdots & \ddots & \vdots \\ \mathbf{T}_{M-1}^H & \mathbf{T}_{M-2}^H & \cdots & \mathbf{T}_0 \end{bmatrix} \tag{10}$$

where $\mathbf{T}_i$ for $i = 0, 1, \ldots, M-1$ is expressed as

$$\mathbf{T}_i = \begin{bmatrix} u_{i,0} & u_{i,-1} & \cdots & u_{i,-(N-1)} \\ u_{i,1} & u_{i,0} & \cdots & u_{i,-(N-2)} \\ \vdots & \vdots & \ddots & \vdots \\ u_{i,N-1} & u_{i,N-2} & \cdots & u_{i,0} \end{bmatrix} \tag{11}$$

After obtaining the optimal noise-free estimate $\tilde{\mathbf{X}}$ of $\hat{\mathbf{X}}$, we combine (2) with (3) to obtain

$$Ivec(\tilde{\mathbf{X}})_{N\times M} = \mathbf{A}(\tilde{\theta})diag(\mathbf{s})\mathbf{B}(\tilde{\varphi})^T \tag{12}$$

where $\tilde{\theta}$ and $\tilde{\varphi}$ denote the estimates of θ and φ. Finally, the estimation problem of DOD and DOA can be solved with the matrix enhancement and matrix pencil (MEMP) method [33].

However, we note that only if $T(\tilde{\mathbf{u}})$ is able to be decomposed into the form of

$$T(\tilde{\mathbf{u}}) = \Psi \Sigma \Psi^H \tag{13}$$

where $\Psi = [\mathbf{b}(\tilde{\varphi}_1)\otimes\mathbf{a}(\tilde{\theta}_1), \mathbf{b}(\tilde{\varphi}_2)\otimes\mathbf{a}(\tilde{\theta}_2), \ldots, \mathbf{b}(\tilde{\varphi}_P)\otimes\mathbf{a}(\tilde{\theta}_P)]$, $\Sigma = diag([\tilde{s}_{l1}, \tilde{s}_{l2}, \ldots, \tilde{s}_{lP}]^T)$, then (8) can be casted to (9) correctly. In fact, (13) does not always hold for twofold block Toeplitz matrices [34], thus, (9) is just an approximation of (8), which will result a decline in estimation accuracy.

To improve the performance of the prime 2D-ANM, we address to solving the problem of (8) in its dual domain, and put forward to a duality-based 2D-ANM algorithm for DOD and DOA estimation, which can avoid the theoretical approximation and the restriction of SMV model.

V. DUALITY-BASED 2D-ANM FOR DOD AND DOA ESTIMATION

A. THE DUAL PROBLEM

To obtain the dual problem of (8), we construct the Lagrangian formulation by augmenting the objective function with a weighted sum of the constraints

$$L(\mathbf{x}_l, \boldsymbol{\alpha}_l, \beta_l) = \|\mathbf{x}_l\|_{\mathcal{A}} + Re[\boldsymbol{\alpha}_l^H(\mathbf{x}_l - \mathbf{U}\mathbf{h}_l - \mathbf{n}_l)] + \beta_l(\mathbf{n}_l^H\mathbf{n}_l - \epsilon^2) \tag{14}$$

where $\boldsymbol{\alpha}_l \in \mathbb{C}^{MN}$ and $\beta_l \in \mathbb{R}^{1+}$ are Lagrange multipliers (or the dual variables) related to the equality and inequality constraints, respectively. The dual function $f(\boldsymbol{\alpha}_l, \beta_l)$ is the infimum of the Lagrangian formulation $L(\mathbf{x}_l, \boldsymbol{\alpha}_l, \beta_l)$ over the optimization variable $\mathbf{h}_l$ and $\mathbf{n}_l$, i.e.

$$\begin{aligned} f(\boldsymbol{\alpha}_l, \beta_l) &= \inf_{\mathbf{h}_l, \mathbf{n}_l} L(\mathbf{x}_l, \boldsymbol{\alpha}_l, \beta_l) \\ &= \inf_{\mathbf{h}_l, \mathbf{n}_l} \Big\{ Re[\boldsymbol{\alpha}_l^H\mathbf{x}_l - \boldsymbol{\alpha}_l^H\mathbf{n}_l] + \beta_l(\mathbf{n}_l^H\mathbf{n}_l - \epsilon^2) \\ &\quad + \|\mathbf{x}_l\|_{\mathcal{A}} - Re[\boldsymbol{\alpha}_l^H\mathbf{U}\mathbf{h}_l] \Big\} \end{aligned} \tag{15}$$

First, minimizing over the unknown noise vector $\mathbf{n}_l \in \mathbb{C}^{MN}$, we can obtain

$$\frac{\partial f(\boldsymbol{\alpha}_l, \beta_l)}{\partial \mathbf{n}_l} = -\boldsymbol{\alpha}_l + 2\beta_l\mathbf{n}_l = 0 \tag{16}$$

Then the optimal noise vector of $\mathbf{n}_l$ is $\mathbf{n}_0 = \boldsymbol{\alpha}_l/(2\beta_l)$. The dual function evaluated at $\mathbf{n}_0$ is

$$f(\boldsymbol{\alpha}_l, \beta_l)|_{\mathbf{n}_0} = Re[\boldsymbol{\alpha}_l^H\mathbf{x}_l] - \frac{\boldsymbol{\alpha}_l^H\boldsymbol{\alpha}_l}{2\beta_l} + \beta_l\Big(\frac{\boldsymbol{\alpha}_l^H\boldsymbol{\alpha}_l}{4\beta_l^2} - \epsilon^2\Big) + \inf_{\mathbf{h}_l}(\|\mathbf{x}_l\|_{\mathcal{A}} - Re[\boldsymbol{\alpha}_l^H\mathbf{U}\mathbf{h}_l]) \tag{17}$$

Next, maximizing the dual function (17) evaluated at the dual variable β_l, we have

$$\frac{\partial f(\boldsymbol{\alpha}_l, \beta_l)}{\partial \beta_l} = \frac{\boldsymbol{\alpha}_l^H\boldsymbol{\alpha}_l}{4\beta_l^2} - \epsilon^2 = 0 \tag{18}$$

Then the optimal value of the dual variable β_l is $\beta_0 = \|\boldsymbol{\alpha}_l\|_2/(2\epsilon)$.

Thus, the dual function at the optimal values $\mathbf{n}_0$ and β_0 becomes

$$f(\boldsymbol{\alpha}_l)|_{\mathbf{n}_0,\beta_0} = Re[\boldsymbol{\alpha}_l^H\mathbf{x}_l] - \epsilon\|\boldsymbol{\alpha}_l\|_2 + \inf_{\mathbf{h}_l}\Big(\|\mathbf{x}_l\|_{\mathcal{A}} - Re[\boldsymbol{\alpha}_l^H\mathbf{U}\mathbf{h}_l]\Big) \tag{19}$$

Finally, we formulate the dual problem of (8) by maximizing the dual function $f(\boldsymbol{\alpha}_l)|_{\mathbf{n}_0,\beta_0}$ over the dual variable $\boldsymbol{\alpha}_l$.

Let h_{li} denote the i-th element of $\mathbf{h}_l$, we note that for each h_{li}, $Re[(\boldsymbol{\alpha}_l^H\mathbf{U})_i h_{li}] = Re[(\mathbf{U}^H\boldsymbol{\alpha}_l)_i^H h_{li}] = |(\mathbf{U}^H\boldsymbol{\alpha}_l)_i||h_{li}|\cos(\phi_i)$, where ϕ_i is the angle between h_{li} and $(\mathbf{U}^H\boldsymbol{\alpha}_l)_i$. Then

$$\begin{aligned} |h_{li}| - Re[(\mathbf{U}^H\boldsymbol{\alpha}_l)_i^H h_{li}] &= |h_{li}|[1 - |(\mathbf{U}^H\boldsymbol{\alpha}_l)_i|\cos(\phi_i)] \\ &\geq |h_{li}|[1 - |(\mathbf{U}^H\boldsymbol{\alpha}_l)_i|] \end{aligned} \tag{20}$$

The lower bound (20) is nonnegative if $|(\mathbf{U}^H\boldsymbol{\alpha}_l)_i| \leq 1$ and the infimum is zero. Otherwise, if $|(\mathbf{U}^H\boldsymbol{\alpha}_l)_i| > 1$, the infimum is attained at $-\infty$. Therefore, the dual function in (19) becomes

$$f(\boldsymbol{\alpha}_l) = \begin{cases} Re[\boldsymbol{\alpha}_l^H\mathbf{x}_l] - \epsilon\|\boldsymbol{\alpha}_l\|_2\,, & \|\mathbf{U}^H\boldsymbol{\alpha}_l\|_\infty \leq 1 \\ -\infty & otherwise \end{cases} \tag{21}$$

According (20), we can also have

$$\begin{aligned} |(\mathbf{U}^H\boldsymbol{\alpha}_l)_i| &= 1, \quad \mathbf{h}_{li} \neq 0 \\ |(\mathbf{U}^H\boldsymbol{\alpha}_l)_i| &< 1, \quad \mathbf{h}_{li} = 0 \end{aligned} \tag{22}$$

Thus, maximizing (21) over $\boldsymbol{\alpha}_l$ constitutes the following dual problem:

$$\begin{aligned} &\max_{\boldsymbol{\alpha}_l \in \mathbb{C}^{MN}} Re[\boldsymbol{\alpha}_l^H\mathbf{x}_l] - \epsilon\|\boldsymbol{\alpha}_l\|_2 \\ &s.t.\ \|\mathbf{U}^H\boldsymbol{\alpha}_l\|_\infty \leq 1 \end{aligned} \tag{23}$$

B. CONVERTING THE DUAL PROBLEM INTO SEMI-DEFINITE PROGRAMMING

The dual problem in (23) is a semi-infinite programming problem with a finite number of optimization variables $\boldsymbol{\alpha}_l \in \mathbb{C}^{MN}$, and infinitely many inequality constraints, which is still intractable.

Fortunately, the inequality constraint in (23) implies that the dual polynomial has amplitude uniformly bounded for all $\mathbf{U}_i \in \mathcal{A}$, then the constraint in (23) can be replaced with finite dimensional linear matrix inequalities. Thus, the dual problem could be solved by semi-definite programming (SDP) [35].

According to (23), we obtain

$$\mathbf{U}_i^H\boldsymbol{\alpha}_l\boldsymbol{\alpha}_l^H\mathbf{U}_i \leq 1 \tag{24}$$

Therefore, we can construct a Hermitian matrix $\mathbf{D}_l \in \mathbb{C}^{MN\times MN}$, which satisfies that for any $\mathbf{U}_i \in \mathcal{A}$, $\mathbf{U}_i^H\mathbf{D}_l\mathbf{U}_i = 1$.

According to the Schur complement, we have

$$\begin{bmatrix} \mathbf{D} & \boldsymbol{\alpha}_l \\ \boldsymbol{\alpha}_l^H & 1 \end{bmatrix} \geq 0 \tag{25}$$

Then (23) is transformed to

$$\begin{aligned} &\max_{\boldsymbol{\alpha}_l \in \mathbb{C}^{MN}, \mathbf{D}_l} Re[\boldsymbol{\alpha}_l^H \mathbf{x}_l] - \epsilon \|\boldsymbol{\alpha}_l\|_2 \\ &s.t. \begin{bmatrix} \mathbf{D}_l & \boldsymbol{\alpha}_l \\ \boldsymbol{\alpha}_l^H & 1 \end{bmatrix} \geq 0 \end{aligned} \tag{26}$$

Similar to (24), when considering the observed matrix $\mathbf{X}$ in (4) with L snapshots, we can also obtain

$$\mathbf{U}_i^H \boldsymbol{\alpha} \boldsymbol{\alpha}^H \mathbf{U}_i \leq L = \mathbf{U}_i^H \mathbf{D} \mathbf{U}_i \tag{27}$$

where $\boldsymbol{\alpha} = [\boldsymbol{\alpha}_1, \boldsymbol{\alpha}_2, \cdots, \boldsymbol{\alpha}_L]$, $\mathbf{D}$ is a newly constructed Hermitian matrix. The details of constructing the matrix $\mathbf{D}$ is elaborated in Section V-C.

Then (26) can be modified as

$$\begin{aligned} &\max_{\boldsymbol{\alpha} \in \mathbb{C}^{MN \times L}, \mathbf{D}} Re[Tr(\boldsymbol{\alpha}^H \mathbf{X})] - \epsilon \|\boldsymbol{\alpha}\|_{2,1} \\ &s.t. \begin{bmatrix} \mathbf{D} & \boldsymbol{\alpha} \\ \boldsymbol{\alpha}^H & \mathbf{I}_L \end{bmatrix} \geq 0 \end{aligned} \tag{28}$$

where $\|\boldsymbol{\alpha}\|_{2,1}$ denotes the sum of the ℓ_2 norms of the columns of the matrix.

C. CONSTRUCTING THE MATRIX D

The details of constructing the matrix $\mathbf{D}$ are as follows:

First, divide the Hermitian matrix $\mathbf{D}$ into an $M \times M$ block matrix, each block is an $N \times N$ matrix. So, $\mathbf{D}$ is expressed as

$$\mathbf{D} = \begin{bmatrix} \mathbf{D}_{0,0} & \mathbf{D}_{0,1} & \cdots & \mathbf{D}_{0,M-1} \\ \mathbf{D}_{0,1}^H & \mathbf{D}_{1,1} & \cdots & \mathbf{D}_{1,M-1} \\ \vdots & \vdots & \ddots & \vdots \\ \mathbf{D}_{0,M-1}^H & \mathbf{D}_{1,M-1}^H & \cdots & \mathbf{D}_{M-1,M-1} \end{bmatrix} \tag{29}$$

Then, we denote

$$\mathbf{T}_j = \sum_{i=0}^{M-1-j} \mathbf{D}_{i,i+j}, \quad j = 0, 1, \ldots, M-1 \tag{30}$$

If $\mathbf{T}$ satisfies that

$$\begin{aligned} &sum(diag(\mathbf{T}_0, 0)) = L \\ &sum(diag(\mathbf{T}_0, k)) = 0, \quad k = 1, \ldots, (N-1) \\ &sum(diag(\mathbf{T}_j, k)) = 0, \quad j = 1, \ldots, (M-1) \\ &\qquad k = -(N-1), \ldots, -1, 0, 1, \ldots, (N-1) \end{aligned} \tag{31}$$

Then, for any $\mathbf{U}_i$, we will have $\mathbf{U}_i^H \boldsymbol{D} \mathbf{U}_i = L$. The proof can be found in the Appendix.

D. THE FINAL OBJECTIVE FUNCTION

Considering the constraint of the matrix $\mathbf{D}$, the final objective function becomes

$$\begin{aligned} &\max_{\boldsymbol{\alpha} \in \mathbb{C}^{MN \times L}, \mathbf{D}} Re[Tr(\boldsymbol{\alpha}^H \mathbf{X})] - \epsilon \|\boldsymbol{\alpha}\|_{2,1} \\ &s.t. \begin{bmatrix} \mathbf{D} & \boldsymbol{\alpha} \\ \boldsymbol{\alpha}^H & \mathbf{I}_L \end{bmatrix} \geq 0 \\ &\quad \mathbf{D} \quad is \quad Hermitian \\ &\quad sum(diag(\mathbf{T}_0, 0)) = L \\ &\quad sum(diag(\mathbf{T}_0, k)) = 0, \quad k = 1, \ldots, (N-1) \\ &\quad sum(diag(\mathbf{T}_j, k)) = 0, \quad j = 1, \ldots, (M-1) \\ &\qquad\qquad k = -(N-1), \ldots, \\ &\qquad\qquad -1, 0, 1, \ldots, (N-1) \end{aligned} \tag{32}$$

Thus, (32) can be solved by off-the-shelf solvers such as SDPT3 [36].

E. ESTIMATING DOD AND DOA FOR MIMO RADAR

After obtaining the optimal estimate $\tilde{\boldsymbol{\alpha}}$ of $\boldsymbol{\alpha}$ in (32), we define a spatial spectral function according to (22), which is written as

$$f(\varphi, \theta) \triangleq [\mathbf{b}(\varphi) \otimes \mathbf{a}(\theta)]^H \tilde{\boldsymbol{\alpha}} \tilde{\boldsymbol{\alpha}}^H [\mathbf{b}(\varphi) \otimes \mathbf{a}(\theta)] \tag{33}$$

where $\varphi \in [-\pi/2, \pi/2)$ and $\theta \in [-\pi/2, \pi/2)$. Then, the locations of the P largest peaks of $f(\varphi, \theta)$ represent the estimated DOD and DOA for the P targets.

VI. DISCUSSION

A. NON-ULA CASE

The proposed 2D-ANM-duality algorithm is also applicable to the non-ULA case. We see that if the elementary positions of non-ULA are the integer multiple of unit distance (with the first element being a reference one), then it can be equivalent to a ULA whose elementary spacing is unit distance, with some array elements being inactive. Then we can add some constraints to the dual parameter matrix $\boldsymbol{\alpha}$. That is, $\boldsymbol{\alpha}_{inactive}$ ($\boldsymbol{\alpha}_{inactive} \in \boldsymbol{\alpha}$) matched with the inactive array elements can be set to zero. Thus, (28) can be rewritten as

$$\begin{aligned} &\max_{\boldsymbol{\alpha} \in \mathbb{C}^{MN \times L}, \mathbf{D}} Re[Tr(\boldsymbol{\alpha}^H \mathbf{X})] - \epsilon \|\boldsymbol{\alpha}\|_{2,1} \\ &s.t. \begin{bmatrix} \mathbf{D} & \boldsymbol{\alpha} \\ \boldsymbol{\alpha}^H & \mathbf{I}_L \end{bmatrix} \geq 0 \\ &\boldsymbol{\alpha}_{inactive} = 0 \end{aligned} \tag{34}$$

B. COMPLEXITY COMPARISON

The computational complexity of the proposed 2D-ANM-duality algorithm can be analyzed and compared with five previously proposed DOD and DOA estimation methods in bistatic MIMO radar, including the 2D-MUSIC [7], 2D-ESPRIT [8], 2D-EM [10], 2D-LASSO [20] and primal 2D-ANM [31]. For the 2D-MUSIC, the computational complexity is $\mathcal{O}\{LM^2N^2 + M^3N^3 + U_m V_m (MN - P)(MN + 1)\}$, where U_m and V_m are the step sizes of DOD and DOA peak searching, respectively. For the 2D-ESPRIT, it requires

$\mathcal{O}\{LM^2N^2+M^3N^3+2P^2(M-1)N+2P^2(N-1)M+6P^3\}$. For the 2D-EM, the complexity is $O\{J_eLMN + J_eP(MN + 2L(MN)^2 + U_e(MN)^3 + V_e(MN)^3)\}$, where J_e is the number of iterations, U_e and V_e denote the step sizes of DOD and DOA peak searching, respectively. For the 2D-LASSO, the complexity is $\mathcal{O}\{LMN(U_lV_l)^2 + L(U_lV_l)^3\}$ [39]–[41], where U_l and V_l respectively denote the numbers of DOD and DOA searching grids. For the 2D-ANM, the complexity is $\mathcal{O}\{(MN+1)^3J_a + M^2N^2 + M^3N^3\}$ [33]–[42], where J_a denotes the number of iterations. For the proposed 2D-ANM-Duality, the complexity is $\mathcal{O}\{(MN+L)^3J_d + U_dV_dL(MN+1)\}$, where J_d is the number of iterations, and U_d and V_d respectively denote the step sizes of DOD and DOA peak searching using the spatial spectral function in (33).

VII. SIMULATION RESULTS

This section shows the simulation results to evaluate the performance of the proposed 2D-ANM-duality algorithm for DOD and DOA estimation in bistatic MIMO radar. The calculation of Cramér-Rao bound (CRB) can be referenced in [37], [38]. The root mean square error (RMSE) is examined at $Q = 200$ Monte Carlo trials, which is defined as

$$RMSE = \frac{1}{P}\sum_{i=1}^{P}\sqrt{\frac{1}{Q}\sum_{j=1}^{Q}[(\tilde{\varphi}_{i,j}-\varphi_i)^2+(\tilde{\theta}_{i,j}-\theta_i)^2]} \quad (35)$$

A. EXAMPLE 1

In this example, we validate the effectiveness of the proposed 2D-ANM-duality algorithm for DOD and DOA estimation. Assume that the numbers of the transmitting and receiving antennas are $M = 10$ and $N = 10$. Two ULAs are used as the transmitting and receiving arrays, with elementary spacings being $d_t = d_r = \lambda/2$, respectively. There are $P = 3$ uncorrelated far-field targets located at $(\varphi, \theta) = (-10°, -20°)$, $(10°, 0°)$, $(30°, 20°)$. The SNR is 5dB. Fig. 2 shows the simulation results of the proposed algorithm under the condition of single snapshot ($L = 1$) and multiple snapshots ($L = 20$), respectively.

It indicates from Fig. 2 that the proposed algorithm can effectively estimate the three targets with high accuracy. Unlike the primal 2D-ANM method which is limited to SMV model with $L = 1$, the proposed method is also applicable for MMV model with $L > 1$. Thus, the multiple-snapshot data can be exploited and the estimation performance can be improved.

B. EXAMPLE 2

In this example, we further explore the capability of the proposed 2D-ANM-duality algorithm in estimating DOD and DOA with non-ULAs. Assume that $M = 10$ and $N = 10$. The positions of two non-ULAs as transmitting and receiving arrays are denoted as $[0, d_t, 2d_t, 4d_t, 6d_t, 7d_t, 8d_t, 10d_t, 12d_t, 13d_t]$ and $[0, 2d_r, 3d_r, 4d_r, 5d_r, 7d_r, 9d_r, 10d_r, 11d_r, 13d_r]$, respectively. Other simulation conditions are the same with VII-A. Based on the optimization function for the non-ULA case in (34), we can obtain the simulation results of DOD and DOA estimation, as shown in Fig. 3.

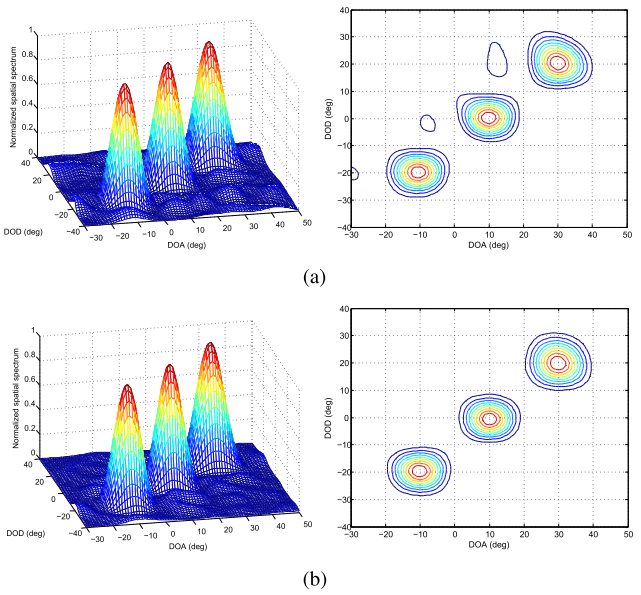

FIGURE 2. Simulation results of estimating DOD and DOA using the proposed algorithm with ULAs. (a) Single snapshot. (b) Multiple snapshots.

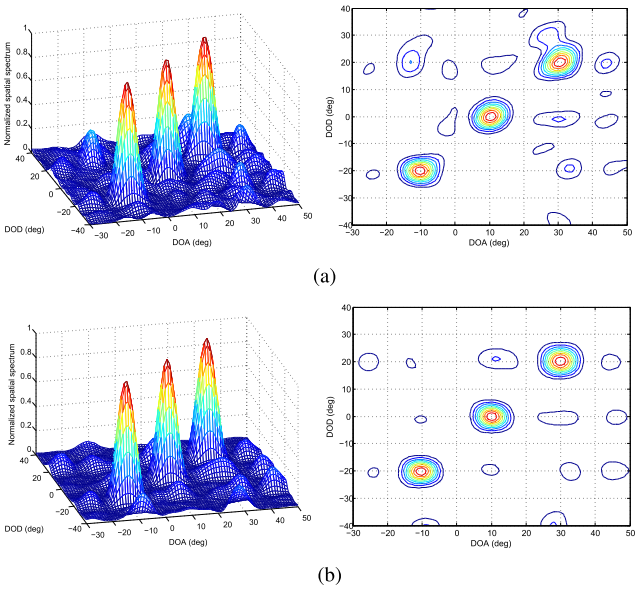

FIGURE 3. Simulation results of estimating DOD and DOA using the proposed algorithm with Non-ULAs. (a) Single snapshot. (b) Multiple snapshots.

From Fig. 3 we can see that the proposed algorithm can effectively estimate DOD and DOA of the three targets with non-ULAs. Unlike the primal 2D-ANM with MEMP, our duality-based 2D-ANM algorithm has the ability to work in the non-ULA case with some elementary spacings larger than half-wavelength.

C. EXAMPLE 3

In this example, we investigate the RMSE performance of the proposed 2D-ANM-duality algorithm for DOD and DOA

estimation in single-snapshot environment, i.e., $L = 1$, and compare our algorithm with the 2D-MUSIC, 2D-ESPRIT, 2D-EM, 2D-LASSO and primal 2D-ANM methods. Assume that $M = 10$ and $N = 10$, with ULA elementary spacings being $d_t = d_r = \lambda/2$. There are $P = 3$ uncorrelated far-field targets located at $(\varphi, \theta) = (-10°, -20°)$, $(10°, 0°)$, $(30°, 20°)$. For the 2D-LASSO, assume that the uniform searching dictionaries of DOD and DOA are $[-30° : 3° : 50°]$ and $[-40° : 3° : 40°]$, respectively, with gird interval 3°. For the 2D-EM, assume that the initial values of DOD and DOA of three targets are $(\varphi_{initial}, \theta_{initial}) = (-5°, -15°)$, $(15°, 5°)$ and $(35°, 25°)$, respectively, and the number of iteration is 200. For the 2D-MUSIC, 2D-EM methods and the proposed algorithm, the step sizes of DOD and DOA peak searching are all 0.2° and the searching ranges are the same with the 2D-LASSO. The results of RMSE versus SNR for the six methods as well as the CRB are shown in Fig. 4.

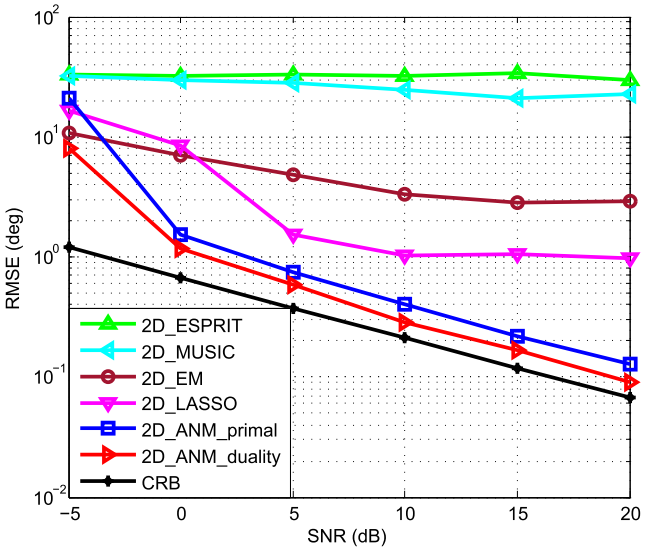

FIGURE 4. RMSE versus SNR in single-snapshot environment ($L = 1$).

From Fig. 4, we can see that the proposed algorithm has the best performance in single-snapshot environment. The subspace-based 2D-MUSIC and 2D-ESPRIT methods have lost the estimation effect with a single snapshot, due to the rank deficiency of the covariance matrices. The 2D-EM requires sufficient snapshots for ML estimation, therefore it cannot achieve higher accuracy in single-snapshot environment. Though the 2D-LASSO as a CS method can work with a single snapshot, its estimation accuracy will degrade due to the grid-mismatch effect. Thus we see that the true values of DOD and DOA do not fall on the grid of the 2D-LASSO, which leads to the deterioration in accuracy, and its RMSE no longer decreases with SNR increasing. The primal 2D-ANM can avoid the grid-mismatch effect as a gridless CS method, however, its estimation accuracy is inferior to the proposed algorithm due to the approximation in the procedure of casting (8) to (9). When the SNR is lower than 0dB, the gap between the proposed algorithm and the primal 2D-ANM method becomes larger. Thus, the proposed 2D-ANM-duality algorithm has the lowest RMSE among the six methods, and its RMSE is close to CRB in single-snapshot environment.

D. EXAMPLE 4

In this example, we investigate the RMSE performance of the proposed 2D-ANM-duality algorithm for DOD and DOA estimation in multiple-snapshot environment. Assume that the number of snapshots is $L = 20$. Other simulation conditions are the same with VII-C. Since the primal ANM method does not work with multiple snapshots, we only compare our algorithm with other four previously proposed DOD and DOA estimation methods, including the 2D-MUSIC, 2D-ESPRIT, 2D-EM and 2D-LASSO. Fig. 5 shows the results of RMSE versus SNR for these five methods.

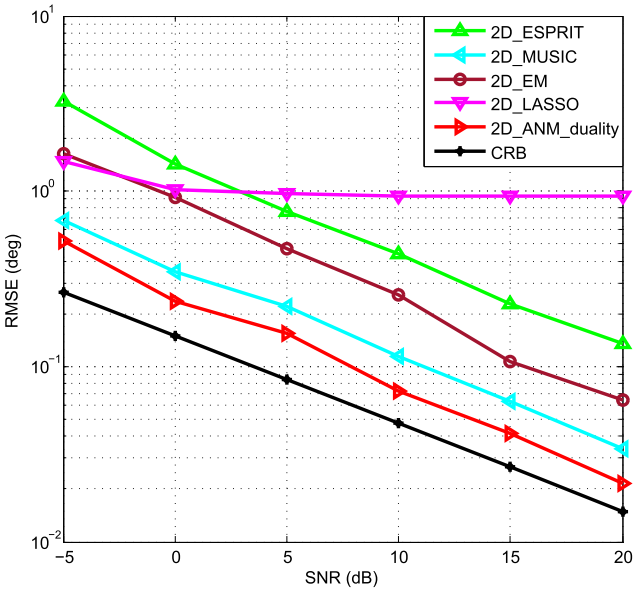

FIGURE 5. RMSE versus SNR in multiple-snapshot environment ($L = 20$).

From Fig. 5 we can observe that the proposed algorithm still has the best performance in multiple-snapshot environment. In the 2D-MUSIC, 2D-ESPRIT and 2D-EM methods, the sample covariance matrices of the observed data are needed for DOD and DOA estimation. When the snapshots is not sufficient ($L = 20$) relative to the product of the numbers of the transmitting and receiving antennas ($MN = 100$), the sample covariance matrices of these methods are no longer the ML estimator of their statistical covariance matrices, which brings to the degradation in estimation performance. In the 2D-LASSO method, the ranges of DOD and DOA are divided into grids for CS dictionary construction and sparse presentation. However, no matter how fine the grid is, the grid-mismatch effect always exists which has reduced its estimation accuracy though the MMV model is used. Also, the computational complexity and the coherence of grids in the 2D-LASSO will greatly increase if the grid interval becomes smaller. In the proposed algorithm, no sample covariance matrix calculation is required, and the

signal can be reconstructed via the continuous domain CS without discrete grid. In addition, the ANM-based method has the function of de-noising. Thus, the proposed algorithm outperforms the subspace-based methods and the grid-based CS methods in estimation accuracy in both single-snapshot and multiple-snapshot environment.

E. EXAMPLE 5

In this example, we investigate the performance of RMSE versus snapshots of the proposed algorithm for DOD and DOA estimation, and compare it with the 2D-MUSIC, 2D-ESPRIT, 2D-EM, 2D-LASSO methods when snapshots L changing from 5 to 25. SNR=5dB. Other simulation conditions are the same with VII-D. The results are shown as Fig. 6. We can see that the proposed algorithm has the best performance among the five methods. From VII-C, VII-D and VII-E, we have verified the advantage of estimation accuracy of the proposed method in different SNR and snapshots.

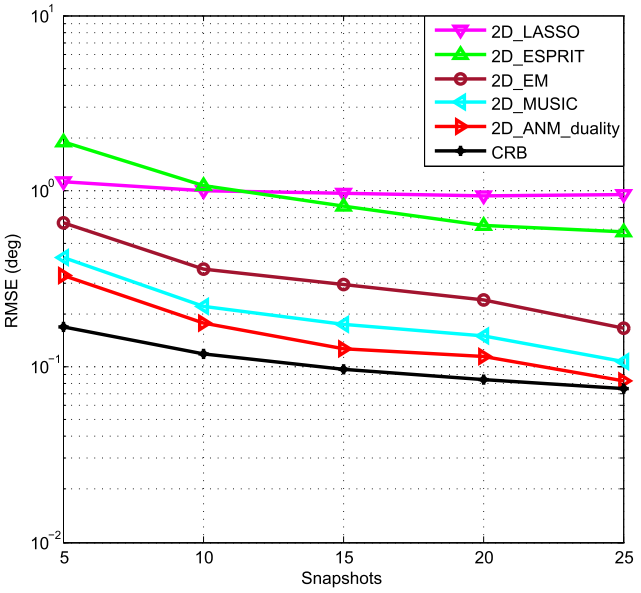

FIGURE 6. RMSE versus snapshots.

F. EXAMPLE 6

In this example, we validate and compare the resolution of DOD and DOA estimation using the proposed 2D-ANM-duality algorithm and 2D-MUSIC, 2D-ESPRIT, 2D-EM, 2D-LASSO methods. Assume that there are two closely spaced targets located at $(\varphi, \theta) = (10°, 20°), (15°, 25°)$. Other simulation conditions are the same with VII-D. The results are shown as Fig. 7 . We can see that the proposed algorithm has higher resolution than other methods in distinguish two closely spaced targets.

G. EXAMPLE 7

In the example, we explore the ability of estimating DOD and DOA of coherent targets using the proposed

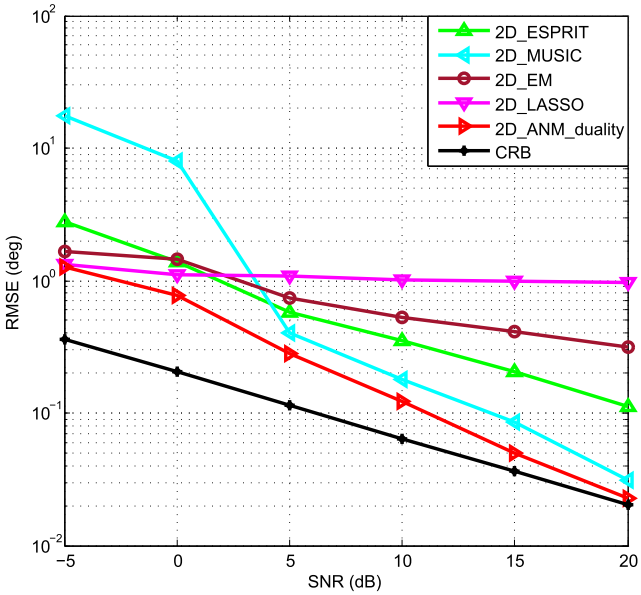

FIGURE 7. RMSE versus SNR with two closely spaced targets.

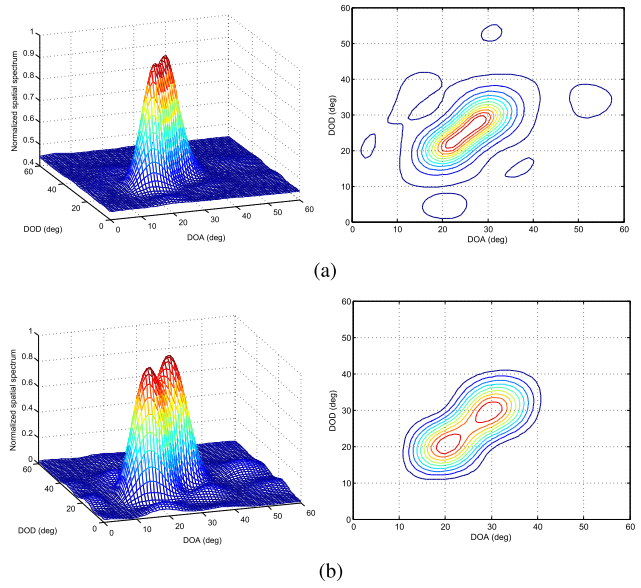

FIGURE 8. Simulation results of estimating DOD and DOA of two coherent targets using the proposed algorithm and the subspace-based 2D-MUSIC method. (a) 2D-MUSIC. (b) 2D-ANM-duality.

2D-ANM-duality algorithm and the 2D-MUSIC method. There are $P = 2$ coherent far-field targets. The second target signal is generated by the first target multiplied by a complex scalar. They are located at $(\varphi, \theta) = (20°, 20°), (30°, 30°)$. The number of snapshots is $L = 20$ and SNR $= 5$dB. Other simulation conditions are same with VII-A. Fig. 8 shows the simulation results of estimating DOD and DOA using the proposed algorithm and the 2D-MUSIC method.

Fig. 8 demonstrates that the proposed algorithm can accurately estimate the DOD and DOA of the two coherent targets. However, the subspace-based 2D-MUSIC cannot distinguish

the two peaks of spatial spectrum, it is not appropriate for the case of target coherence.

H. EXAMPLE 8

In the final example, we make a comparison of computational complexity of the proposed 2D-ANM-duality algorithm with the 2D-MUSIC, 2D-ESPRIT, 2D-EM, 2D-LASSO and primal 2D-ANM methods in single-snapshot environment. Since there are undetermined numbers of iterations for the 2D-LASSO, 2D-ANM and 2D-ANM-duality in noisy environment, we compare the six methods in term of the average running time in 200 Monte Carlo trials, based on Windows 10, Intel(R) Core(TM) i5-8250U CPU @ 1.60GHz 1.80GHz, RAM 8GB. The simulation conditions are the same with VII-C. The average running time is shown in Table. 1.

TABLE 1. Running time.

Methods	Running time (s)
2D-ESPRIT	0.273119
2D-ANM-primal	7.029723
2D-MUSIC	10.926102
2D-LASSO	12.757678
2D-ANM-duality	15.121084
2D-EM	15.164405

From Table. 1 we can see that the 2D-ESPRIT has the lightest computational burden, followed by the primal 2D-ANM, 2D-MUSIC and 2D-LASSO. The proposed algorithm and the 2D-EM method have heavier computational cost, and they are similar in running time.

VIII. CONCLUSION

In this paper, a novel grid-free DOD and DOA estimation algorithm is proposed for bistatic MIMO radar via duality-based 2D-ANM. The problem of solving 2D-ANM is formulated, and the procedure of converting the primal 2D-ANM into its dual problem is derived. The proposed algorithm outperforms the primal 2D-ANM in estimation accuracy. It works well in both cases of a single measurement and multiple measurements, and is also appropriate for the non-ULAs. It achieves robust estimation performance in contrast to the subspace-based methods in target coherence and single-snapshot environment. In addition, compared with the conventional CS methods, the proposed algorithm is not affected by the grid mismatch effect, thus high accuracy can be obtained.

APPENDIX

THE PROOF

$$[\mathbf{b}(\varphi)\otimes\mathbf{a}(\theta)]^H\mathbf{D}[\mathbf{b}(\varphi)\otimes\mathbf{a}(\theta)] = sum\{[\mathbf{b}(\varphi)\otimes\mathbf{a}(\theta)]^*[\mathbf{b}(\varphi)\otimes\mathbf{a}(\theta)]^T\odot\mathbf{D}\} \tag{36}$$

where $\odot$ denote the Hadamard product. Let $\mathbf{G} = [\mathbf{b}(\varphi)\otimes\mathbf{a}(\theta)]^*[\mathbf{b}(\varphi)\otimes\mathbf{a}(\theta)]^T$. All the elements of $\mathbf{G}$ is exponential. Also, $\mathbf{G}$ is a Hermitian and twofold Toeplitz matrix.

$$\mathbf{G} = \begin{bmatrix} \mathbf{G}_{0,0} & \mathbf{G}_{0,1} & \cdots & \mathbf{G}_{0,M-1} \\ \mathbf{G}_{0,1}^H & \mathbf{G}_{0,0} & \cdots & \mathbf{G}_{0,M-2} \\ \vdots & \vdots & \ddots & \vdots \\ \mathbf{G}_{0,M-1}^H & \mathbf{G}_{0,M-2}^H & \cdots & \mathbf{G}_{0,0} \end{bmatrix} \tag{37}$$

where $\mathbf{G}_{i,j}$ is a Toeplitz matrix. Each diagonal value of $\mathbf{G}_{0,0}$ is one.

When $\mathbf{D}$ is a Hermitian matrix and denoted as

$$\mathbf{D} = \begin{bmatrix} \mathbf{D}_{0,0} & \mathbf{D}_{0,1} & \cdots & \mathbf{D}_{0,M-1} \\ \mathbf{D}_{0,1}^H & \mathbf{D}_{1,1} & \cdots & \mathbf{D}_{1,M-1} \\ \vdots & \vdots & \ddots & \vdots \\ \mathbf{D}_{0,M-1}^H & \mathbf{D}_{1,M-1}^H & \cdots & \mathbf{D}_{M-1,M-1} \end{bmatrix} \tag{38}$$

Let

$$\mathbf{T}_j = \sum_{i=0}^{M-1-j} \mathbf{D}_{i,i+j}, \quad j = 0, 1, \cdots, M-1 \tag{39}$$

If $\mathbf{T}$ satisfies

$$\begin{aligned} &sum(diag(\mathbf{T}_0, 0)) = L \\ &sum(diag(\mathbf{T}_0, k)) = 0, k = 1, \cdots, (N-1) \\ &sum(diag(\mathbf{T}_j, k)) = 0, j = 1, \cdots, (M-1) \\ &\qquad k = -(N-1), \cdots, -1, \quad 0, 1, \cdots, (N-1) \end{aligned} \tag{40}$$

Then, we can obtain $sum(\mathbf{G}\odot\mathbf{D}) = L$, that is $[\mathbf{b}(\varphi)\otimes\mathbf{a}(\theta)]^H\mathbf{D}[\mathbf{b}(\varphi)\otimes\mathbf{a}(\theta)] = L$. For any $\mathbf{U}_i \in \mathcal{A}$, from (5), we have $\mathbf{U}_i^H\boldsymbol{D}\mathbf{U}_i = L$.

REFERENCES

[1] E. Fishler, A. Haimovich, R. Blum, D. Chizhik, L. Cimini, and R. Valenzuela, "MIMO radar: An idea whose time has come," in *Proc. IEEE Radar Conf.*, Philadelphia, PA, USA, Apr. 2004, pp. 71–78,.

[2] C. Zhang, H. Huang, and B. Liao, "Direction finding in MIMO radar with unknown mutual coupling," *IEEE Access*, vol. 5, pp. 4439–4447, 2017.

[3] L. Xu, J. Li, and P. Stoica, "Target detection and parameter estimation for MIMO radar systems," *IEEE Trans. Aerosp. Electron. Syst.*, vol. 44, no. 3, pp. 927–939, Jul. 2008.

[4] Z. Wang, W.-Q. Wang, and H. Shao, "MIMO radar using frequency incremental waveforms for range-angle localization of targets," in *Proc. Int. Conf. Radar Syst. (Radar)*, Belfast, U.K., 2017, pp. 1–4.

[5] J. Li and P. Stoica, *MIMO Radar Signal Processing*. Hoboken, NJ, USA: Wiley, 2009.

[6] H. Yan, J. Li, and G. Liao, "Multitarget identification and localization using bistatic MIMO radar systems," *EURASIP J. Adv. Signal Process.*, vol. 2008, no. 1, 2007, Art. no. 283483.

[7] X. F. Zhang, L. Y. Xu, L. Xu, and D. Z. Xu, "Direction of departure (DOD) and direction of arrival (DOA) estimation in MIMO radar with reduced-dimension MUSIC," *IEEE Commun. Lett.*, vol. 14, no. 12, pp. 1161–1163, Dec. 2010.

[8] C. Duofang, C. Baixiao, and Q. Guodong, "Angle estimation using ESPRIT in MIMO radar," *Electron. Lett.*, vol. 44, no. 12, pp. 770–771, Jun. 2008.

[9] M. Jin, G. S. Liao, and J. Li, "Joint DOD and DOA estimation for bistatic MIMO radar," *Signal Process.*, vol. 89, no. 2, pp. 244–251, Feb. 2009.

[10] H. W. Chen, D. Yang, H.-Q. Wang, X. Li, and Z. Zhuang, "Direction finding for bistatic MIMO radar using EM maximum likelihood algorithm," *Prog. Electromagn. Res.*, vol. 141, pp. 99–116, Oct. 2013.

[11] A. B. Gershman, M. Rübsamen, and M. Pesavento, "One- and two-dimensional direction-of-arrival estimation: An overview of search-free techniques," *Signal Process.*, vol. 90, no. 5, pp. 1338–1349, 2010.

[12] G. Zheng, J. Tang, and X. Yang, "ESPRIT and unitary ESPRIT algorithms for coexistence of circular and noncircular signals in bistatic MIMO radar," *IEEE Access*, vol. 4, pp. 7232–7240, 2016.
[13] S. Gong, H. Xiong, M. Peng, X. Ding, and H. Tang, "Joint DOD and DOA estimation for bistatic multiple-input multiple-output radar target discrimination based on improved unitary ESPRIT method," *IET Commun.*, vol. 12, no. 12, pp. 1397–1405, Jul. 2018.
[14] D. L. Donoho, "Compressed sensing," *IEEE Trans. Inf. Theory*, vol. 52, no. 4, pp. 1289–1306, Apr. 2006.
[15] E. J. Candès and M. B. Wakin, "An introduction to compressive sampling," *IEEE Signal Process. Mag.*, vol. 25, no. 2, pp. 21–30, Mar. 2008.
[16] C.-Y. Chen and P. P. Vaidyanathan, "Compressed sensing in MIMO radar," in *Proc. 42nd Asilomar Conf. Signals, Syst. Comput.*, Pacific Grove, CA, USA, 2008, pp. 41–44.
[17] Y. Yu, A. P. Petropulu, and H. V. Poor, "Measurement matrix design for compressive sensing–based MIMO radar," *IEEE Trans. Signal Process.*, vol. 59, no. 11, pp. 5338–5352, Nov. 2011.
[18] M. Rossi, A. M. Haimovich, and Y. C. Eldar, "Spatial compressive sensing for MIMO radar," *IEEE Trans. Signal Process.*, vol. 62, no. 2, pp. 419–430, Jan. 2014.
[19] X. Zhao, C. Guo, and W. Peng, "Fast 3D parameters estimation of targets in bistatic MIMO radar based on sparse signal reconstruction," *IEEE Access*, vol. 6, pp. 46206–46212, 2018.
[20] T. Strohmer and B. Friedlander, "Analysis of Sparse MIMO Radar," *Appl. Comput. Harmon. Anal.*, vol. 37, no. 3, pp. 361–388, 2014.
[21] R. Tibshirani, "Regression shrinkage and selection via the lasso: A retrospective," *J. Roy. Stat. Soc., B (Stat. Methodol.)*, vol. 73, no. 3, pp. 1369–7412, 2011.
[22] Y. Chi, L. L. Scharf, A. Pezeshki, and A. R. Calderbank, "Sensitivity to basis mismatch in compressed sensing," *IEEE Trans. Signal Process.*, vol. 59, no. 5, pp. 2182–2195, May 2011.
[23] P. Chen, Z. Cao, Z. Chen, and X. Wang, "Off-grid DOA estimation using sparse Bayesian learning in MIMO radar with unknown mutual coupling," *IEEE Trans. Signal Process.*, vol. 67, no. 1, pp. 208–220, Jan. 2019.
[24] P. Chen, L. Zheng, X. Wang, H. Li, and L. Wu, "Moving Target Detection Using Colocated MIMO Radar on Multiple Distributed Moving Platforms," *IEEE Trans. Signal Process.*, vol. 65, no. 17, pp. 4670–4683, Sep. 2017.
[25] A. Abtahi, S. Gazor, and F. Marvasti, "Off-grid localization in MIMO radars using sparsity," *IEEE Signal Process. Lett.*, vol. 25, no. 2, pp. 313–317, Feb. 2018.
[26] G. Tang, B. N. Bhaskar, P. Shah, and B. Recht, "Compressed sensing off the grid," *IEEE Trans. Inf. Theory*, vol. 59, no. 11, pp. 7465–7490, Nov. 2013.
[27] B. N. Bhaskar, G. Tang, and B. Recht, "Atomic norm denoising with applications to line spectral estimation," *IEEE Trans. Signal Process.*, vol. 61, no. 23, pp. 5987–5999, Dec. 2013.
[28] B. Hu, X. Wu, X. Zhang, Q. Yang, and W. Deng, "Off-grid DOA estimation based on compressed sensing with gain/phase uncertainties," *Electron. Lett.*, vol. 54, no. 21, pp. 1241–1243, 2018.
[29] Z. Yang and L. Xie, "On gridless sparse methods for line spectral estimation from complete and incomplete data," *IEEE Trans. Signal Process.*, vol. 63, no. 12, pp. 3139–3153, Jun. 2015.
[30] Z. Yang and L. Xie, "Continuous compressed sensing with a single or multiple measurement vectors," in *Proc. IEEE Workshop Stat. Signal Process. (SSP)*, Gold Coast, VIC, USA, Jun./Jul. 2014, pp. 288–291.
[31] Y. Yang, Z. Chu, Z. Xu, and G. Ping, "Two-dimensional grid-free compressive beamforming," *J. Acoust. Soc. Amer.*, vol. 142, no. 2, pp. 618–629, 2017.
[32] V. Chandrasekaran, B. Recht, P. A. Parrilo, and A. S. Willsky, "The convex geometry of linear inverse problems," *Found. Comput. Math.*, vol. 12, pp. 805–849, Dec. 2012.
[33] Y. Hua, "Estimating two-dimensional frequencies by matrix enhancement and matrix pencil," *IEEE Trans. Signal Process.*, vol. 40, no. 9, pp. 2267–2280, Sep. 1992.
[34] Y. Chi and Y. Chen, "Compressive two-dimensional harmonic retrieval via atomic norm minimization," *IEEE Trans. Signal Process.*, vol. 63, no. 4, pp. 1030–1042, Feb. 2015.
[35] A. Xenaki and P. Gerstoft, "Grid-free compressive beamforming," *J. Acoust. Soc. Amer.*, vol. 137, no. 4, pp. 1923–1935, 2015.
[36] K. C. Toh, M. J. Todd, and R. H. Tutuncu, "SDPT3—A Matlab software package for semidefinite programming, Version 1.3," *Optim. Methods Softw.*, vol. 11, no. 14, pp. 545–581, 1999.
[37] P. Stoica and R. L. Moses, *Spectral Analysis of Signals*, Upper Saddle River, NJ, USA: Prentice-Hall, 1997. pp. 285–293.
[38] B. Tang, J. Tang, Y. Zhang, and Z. Zheng, "Maximum likelihood estimation of DOD and DOA for bistatic MIMO radar," *Signal Process.*, vol. 93, no. 5, pp. 1349–1357, 2013.
[39] B. Efron, T. Hastie, I. Johnstone, and R. Tibshirani, "Least angle regression," *Ann. Statist.*, vol. 32, no. 2, pp. 407–499, 2004.
[40] M. Schmidt, "Least squares optimization with L1-norm regularization," Univ. British Columbia, Vancouver, BC, Canada, Tech. Rep. CS542B, 2005.
[41] J. Mairal and B. Yu, "Complexity analysis of the lasso regularization path," in *Proc. 29th Int. Conf. Mach. Learn.*, Scotland, UK, 2012, pp. 1–8.
[42] K. Krishnan and T. Terlaky, "Interior point and semidefinite approaches in combinatorial optimization," *Graph Theory and Combinatorial Optimization*. Boston, MA, USA: Springer, 2005, pp. 101–157.

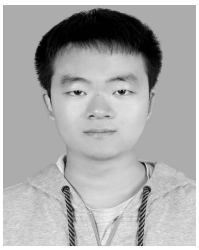

WEN-GEN TANG (S'18) received the B.S. degree from the College of Communication Engineering, Jilin University, Changchun, China, in 2018, where he is currently pursuing the Ph.D. degree in information and communication engineering. His research interests include gridless compressive sensing, sparse signal recovery and their application in array signal processing, parameter estimation, and target localization in multiple-input-multiple-output radar.

HONG JIANG (M'12) received the B.S. degree in radio technology from Tianjin University, Tianjin, China, in 1989, the M.S. degree in communication and electronic systems from the Jilin University of Technology, Changchun, China, in 1996, and the Ph.D. degree in communication and information systems from Jilin University, Changchun, in 2005. From 2010 to 2011, she was a Visiting Scholar with the Department of Electrical and Computer Engineering, McMaster University, Hamilton, ON, Canada. She is currently a Professor with the College of Communication Engineering, Jilin University. Her research interests include array signal processing, signal detection and parameter estimation, target identification and localization in multiple-input-multiple-output radar, and signal processing for wireless communication and localization. She is a Senior Member of the Chinese Institute of Electronics.

SHUAI-XUAN PANG received the B.S. degree from the College of Communication Engineering, Jilin University, Jilin, China, in 2016, where he is currently pursuing the M.S. degree. His research interests include angle-range estimation and target localization in frequency diverse array (FDA) radar.